JOURNAL OF APPLIED ELECTROCHEMISTRY 17 (1987) 532–544

*Electrosynthesis of propylene oxide in a bipolar trickle-bed reactor**

A. MANJI

ERCO Industries Ltd., 2 Gibbs Road, Islington, Ontario, Canada M9B 1RI

C. W. OLOMAN

Department of Chemical Engineering, University of British Columbia, Vancouver, British Columbia, Canada V6T 1W5

Received 25 February 1986; revised 12 May 1986

The synthesis of propylene oxide by electrolysis of dilute sodium bromide solution with propylene gas was investigated in an electrochemical 'flow-by' bipolar reactor consisting of six parallel fixed beds of graphite particles separated by polypropylene felt diaphragms. The reactor was operated in a single pass mode with a two-phase co-current flow of propylene and sodium bromide solution through the beds of graphite particles. The maximum pressure in the system was 2.2 atm absolute.

The effects of superficial current density (0.4–2.7 kA m^{-2}), sodium bromide concentration (0.2 and 0.5 M), electrolyte load (4.4–13.2 kg m^{-2} s^{-1}), propylene gas load (0.08–1.66 kg m^{-2} s^{-1}), reactor outlet temperature (30 and 60° C), bed thickness (5–15 mm) and different carbon types (Union Carbide and Ultra Carbon) on the space–time yield and selectivity for propylene oxide were measured. Depending on conditions, the space–time yield for propylene oxide was between 5.5 and 97 kg m^{-3} h^{-1}, and the selectivity was between 55 and 87%. The current efficiency and the specific energy consumption varied from 14 to 58% and from 6 to 60 kWh kg^{-1} of propylene oxide. The space–time yield for propylene oxide increased with increasing current density, increasing gas flow and decreasing bed thickness.

The current efficiencies for hydrogen, oxygen, dibromopropane, hypobromite, bromite and bromate were also determined.

1. Introduction

There are several published studies of the *in situ* synthesis of propylene oxide from propylene with an alkali halide electrolyte in bipolar electrochemical reactors [1–8]. The major reactions in this process with a bromide electrolyte are understood to be as shown in Equations 1 to 5.

Anode:

$$2Br^- \longrightarrow Br_2 + 2e \qquad (1)$$

$$E_0 = 1.09\,V \text{ versus SHE}$$

Cathode:

$$2H_2O + 2e \longrightarrow H_2 + 2OH^- \qquad (2)$$

$$E_0 = -0.83\,V \text{ versus SHE}$$

Bulk:

$$Br_2 + H_2O + P \longrightarrow PBH \qquad (3)$$

$$PBH + OH^- \longrightarrow H_2O + Br^- + PO \qquad (4)$$

Overall:

$$P + H_2O \xrightarrow{2e} PO + H_2 \qquad (5)$$

Current efficiency and selectivity for propylene oxide are lost by various secondary electrode and bulk reactions, e.g.

Anode:

$$4OH^- \longrightarrow 2H_2O + O_2 + 4e \qquad (6)$$

$$E_0 = 0.40\,V \text{ versus SHE}$$

* Paper first presented at the AIChE Symposium on Electrochemical Reaction Engineering, Seattle, Washington, 15 August 1985.

0021-891X/87 $03.00 + .12

$$60Br^- + 3H_2O \rightarrow 2BrO_3^- + 4Br^- + 6H^+ + \tfrac{3}{2}O_2 + 6e \quad (7)$$

$E_0 = 1.45\,V$ versus SHE

Cathode:

$$Br_2 + 2e \longrightarrow 2Br^- \quad (8)$$

$E_0 = 1.09\,V$ versus SHE

$$OBr^- + H_2O + 2e \rightarrow Br^- + 2OH^- \quad (9)$$

$E_0 = 0.76\,V$ versus SHE

$$O_2 + 2H_2O + 4e \longrightarrow 4OH^- \quad (10)$$

$E_0 = 0.40\,V$ versus SHE

Bulk:

$$2HOBr + OBr^- \longrightarrow BrO_3^- + 2Br^- + 2H^+ \quad (11)$$

$$2OBr^- \longrightarrow 2Br^- + O_2 \quad (12)$$

$$P + Br_2 \longrightarrow DBP \quad (13)$$

$$PO + H_2O \longrightarrow PG \quad (14)$$

plus other organic reactions producing propanol, propyl ethers, etc. [9]. (P, propylene; PBH, propylene bromohydrin; PO, propylene oxide; PG, propylene glycol; DBP, dibromopropane.)

Reactors used in previous studies consist of arrays of solid bipole elements such as individual particles [1], plates [2], rods [3, 7] and Raschig rings [5, 8]. Each element is driven to function as an individual bipole, around which the reactions take place in the proper sequence. The reactor feed may be a saturated solution of propylene in the aqueous alkali halide [7] (usually sodium bromide) or the two separate gas and electrolyte phases, as used in the bipole trickle tower [5, 8]. Although these reactors give high selectivity for propylene oxide, their performance is generally compromised by low space–time yield which typically is up to 10 kg of propylene oxide per hour per m^3 of reactor volume [8]. The low space–time yield is a result of low propylene solubility in the aqueous electrolyte (~ 0.01 M at 25° C and 1 bar absolute) and/or the low rate of absorption of propylene into the electrolyte in the two-phase system.

Apart from raising the process pressure, the propylene transfer constraint in this process may be relieved in a bipolar porous electrode [10] operated as a trickle-bed with high gas and liquid load [11]. Fig. 1 shows the configuration of such a reactor employing four 'flow-by' bipolar trickle-bed electrodes between two monopole beds.

The work described here [12] assessed the performance of a 'flow-by' bipolar trickle-bed

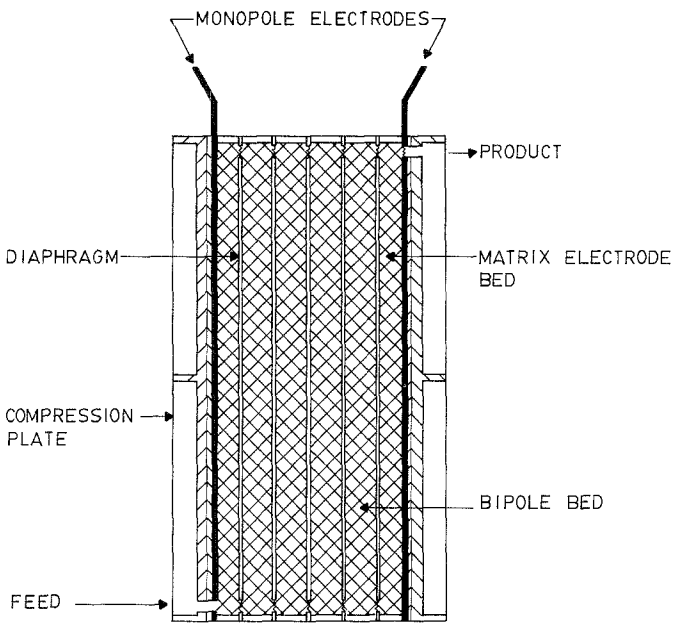

Fig. 1. Vertical cross section of bipolar trickle-bed electrochemical reactor (four bipole beds)

electrochemical reactor for *in situ* synthesis of propylene oxide. A major objective of the study was to find conditions for the production of propylene oxide with high space–time yield.

2. Apparatus and procedure

2.1. *Apparatus*

The bench scale, bipole trickle-bed reactor was constructed as a sandwich of six parallel rectangular beds of graphite particles separated by five diaphragms as in Fig. 1. The monopole feeder electrodes were of platinized titanium, the beds were of graphite particles, 1.2–1.7 mm in diameter, and the diaphragm was of polypropylene felt, 2 mm thick. Each of the graphite beds was held inside neoprene gaskets to give superficial (diaphragm) dimensions of 190 × 25 mm, corresponding to a superficial electrode area per cell of $4.8 \times 10^{-3}\,m^2$. The beds were compressed tightly to minimize the matrix resistivity and the thickness of each of the four bipole beds was adjusted from 5 to 15 mm for different experiments.

The graphite used for the bed material was obtained from two suppliers: (i) Union Carbide Canada Ltd, Toronto, Ontario, Canada, designated as UCAR No. 1 with 0.11% iron and 0.32% ash; (ii) Ultra Carbon Corp., Bay City, Michigan, USA designated UCP 901 chips with 'barely detectable' iron content. Both sets of graphite particles were screened to +1.2–1.7 mm, then treated in hot 1 M hydrochloric acid and rinsed in water to remove residual iron. The rough, porous particles had a specific surface area of about $1\,m^2\,g^{-1}$.

This reactor (A) was disposed in the apparatus shown in Fig. 2. In operation the reactor was fed from the bottom with a mixtue of sodium bromide in water (electrolyte) and propylene gas which flowed co-currently through the electrode matrices. The distribution of liquid and gas between beds from the internal feed manifold was not measured in these runs, but previous (unpublished) tests showed flow differences of about ±20% between cells in a similar multicell reactor. Part of the electrolyte solution was recycled around the feed tank (B) through a heat

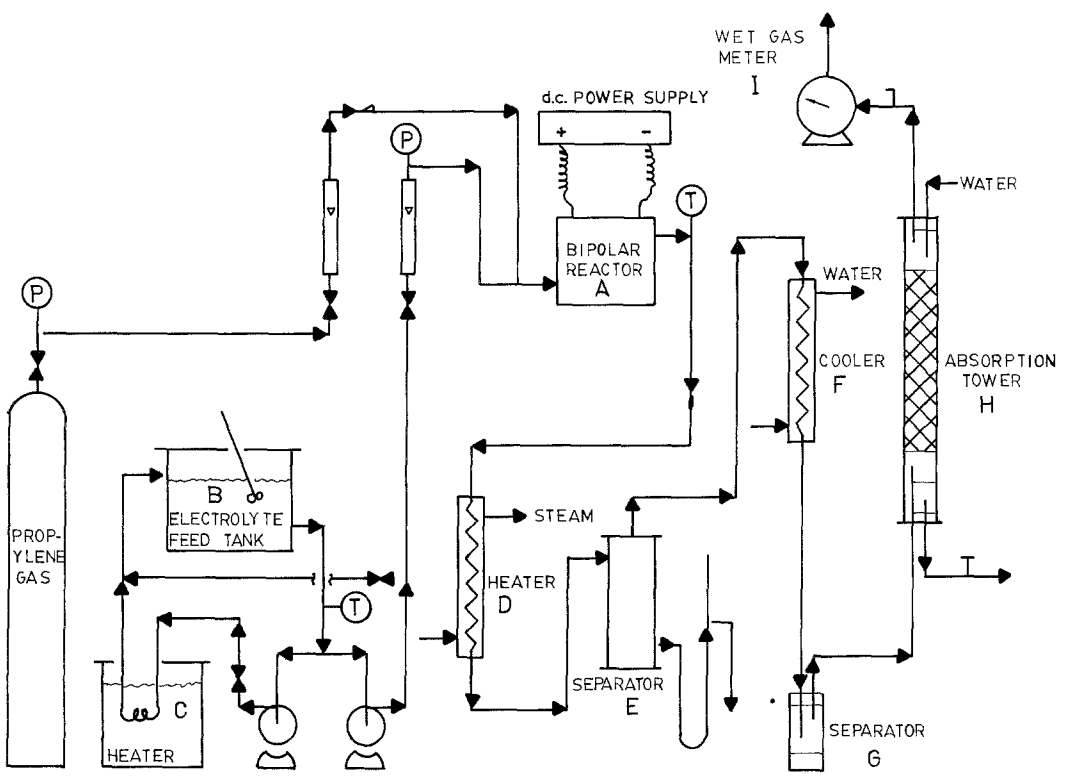

Fig. 2. Flow diagram of apparatus for electrosynthesis of propylene oxide. See text for explanation.

exchanger (C) to control the reactor outlet temperature. The fluid mixture leaving the reactor was passed through a steam heater (D) to strip propylene oxide and then passed into a gas–liquid separator (E). Liquid (spent electrolyte) from the bottom of the separator was disposed to the drain and the gases passed through a condenser (F) against water at about 12° C into a second separator (G). Gas from the second separator was passed through a packed column (H) (60 cm long × 2.5 cm i.d. with 6 mm Berl saddles) countercurrent to 100 $cm^3 min^{-1}$ of water at 12° C and exhausted through a displacement gas flow meter (I).

All parts outside the reactor in contact with the electrolyte were made of stainless steel, nylon, glass, polyethylene or plexiglass. Some corrosion was observed around stainless steel parts after several weeks of use. Power for the reactor was supplied by current control from two Sorensen d.c. power supplies connected in series to supply up to 30 A at 75 V. Electrolyte solutions were made with 99% sodium bromide (BDH Company) in deionized water, and propylene gas was C.P. grade 99% purity (Canadian Liquid Air).

2.2. *Operation*

Experimentation consisted of a series of 150 single-pass runs in which measurements were made on the feed sodium bromide concentration, electrolyte and propylene feed rates, electrolyte temperature entering and leaving the reactor, electrolyte pH leaving the first separator (Fig. 2, E), reactor inlet pressure, voltage and current.

Results were obtained by measuring the various flows and compositions discussed in Section 2.3 below.

2.3. *Analysis*

The flows of gas and liquid from the absorption column and liquid from the second separator were measured. The propylene oxide content of these streams was measured using a gas–liquid chromatograph at 80° C (Varian Model 1400) with flame ionization detector. The column packing was Carbopak C 80/100 coated with 0.2% CW 1500 and the carrier gas was helium. Product gas was also analysed for hydrogen and oxygen in a separate gas chromatograph (Hewlett Packard Model 5710) with a thermal conductivity detector, molecular sieve packing and Argon carrier gas.

Dibromopropane forms a separate phase in the second separator (Fig. 2, G) and was separated and measured by means of a microsyringe. Dissolved dipromopropane in the second separator was determined by extraction with ether in a few runs, and this concentration was assumed constant for the aqueous phase in contact with undissolved dibromopropane.

Hypobromite, bromite and bromate concentrations in the spent electrolyte leaving the first separator were analysed using the standard iodiometric titrations with ammonium sulphate [13].

3. Results and discussion

A list of the independent and dependent variables examined in this work is given in Table 1. Values of the dependent variables were calculated from product analyses and flows by the following relations.

$$\text{Space–time yield for PO} = \frac{\text{Rate of PO production}}{\text{Total volume of five beds + diaphragms but excluding gaskets and feeder electrodes}}$$

$$\text{Selectivity for PO} = \frac{\text{Rate of PO production}}{\text{Rate of PO + DBP production}}$$

$$\text{Current efficiency } (CE) = \frac{\text{Rate of PO production} \times nF}{5I}$$

$$\text{Specific energy for PO} = \frac{26.8nV}{58CE} \text{ kW h per kg of PO}$$

where production rates are in g mol s^{-1}; n = number of electrons in reaction stoichiometry = 2; I = total current to reactor (A); V = reactor voltage per cell (V).

Table 1. List of independent and dependent variables

Variables	*Levels*
Independent	
a, Reactor outlet temperature (°C)	30 and 60
b, Current (A)	2 and 5
c, Electrolyte concentration (M)	0.2 and 0.5
d, Electrolyte flow rate ($cm^3 min^{-1}$)	100 and 300
e, Propylene gas flow rate ($cm^3 min^{-1}$) STP	100–2000
f, Bipole bed thickness (mm)	15–5
g, Bipole bed material	UCAR and Ultra-carbon + 1.2–1.7 mm diameter porous graphite particles
Dependent	
Space–time yield for propylene oxide	
Selectivity for propylene oxide	
Current efficiency for propylene oxide	
Current efficiency for dibromopropane	
Current efficiency for hydrogen and oxygen	
Current efficiency for bromates, bromite and hypobromite	
Specific energy consumption for propylene oxide	

The performance of the bipole trickle-bed reactor in the electrosynthesis of propylene oxide depends on a complex interaction of the effects of the independent variables listed in Table 1. A mechanistic description of the process is outside the scope of this work, but the data can be rationalized in terms of the following qualitative process description.

When the graphite particle beds are sufficiently compressed each behaves as a nearly isopotential electronic conductor. A potential gradient in the electrolyte across the bed sets up an electrochemical cell between opposite faces of the bed which is sustained by electrolytic current 'bypass' through liquid held up in the bed. Current bypass is a major source of lost current efficiency, whose extent depends on the bed thickness, current density and effective conductivity of the electrolyte, which in turn is a function of electrolyte concentration and liquid hold-up in the bed.

Apart from current bypass, current efficiency for propylene oxide is lost through secondary electrode reactions such as Reactions 6–10, together with inefficiencies caused by lack of selectivity in the bulk reaction. These effects are governed by the current density, intra-cell and inter-cell mixing, mass transfer (of bromide and propylene) and reaction temperature through their influence on the relative rates of the electrode and bulk reactions.

A further consideration is the fact that opposite faces of each bed operate as three-dimensional electrodes whose effectiveness is a function of superficial current density, reactant concentration and effective electrolyte conductivity. These factors are tied to the space–time yield through the effect of gas and liquid load on mass transfer and liquid hold-up in the bipole bed.

Specific energy for propylene oxide depends inversely on current efficiency and directly on reactor voltage. The voltage drop across the diaphragms can be a substantial component of the reactor voltage, depending on the liquid hold-up in the diaphragm.

The experimentally observed effects of the independent variables on reactor performance are summarized in Tables 2–6 and graphs of Figs 3 and 4. Fluid flows are given in Tables 2, 3, 4, 6, 8 and Fig. 3 as loadings based on the superficial flow area of the electrode beds normal to the current, and the currents are given as superficial current densities based on the diaphragm area per cell. Corresponding values of the measured variables in the 15 mm thick beds are as follows. Liquid, $4.4\,kg\,m^{-2}s^{-1} \cong 0.11\,min^{-1}$; gas, $0.83\,kg\,m^{-2}s^{-1} \cong 1.01\,min^{-1}$ STP; current, $1\,kA\,m^{-2} \cong 5\,A$.

Table 2. Factorial experiment results

	Reactor outlet, 30° C				*Reactor outlet, 60° C*			
	0.4 kA m^{-2}		*1 kA m^{-2}*		*0.4 kA m^{-2}*		*1 kA m^{-2}*	
	0.2 M NaBr	*0.5 M NaBr*	*0.2 M NaBr*	*0.5 M NaBr*	*0.2 M NaBr*	*0.5 M NaBr*	*0.2 M NaBr*	*0.5 M NaBr*
Electrolyte load, 13.2 kg m^{-2} s^{-1}	12.4[a]	14.8	30.5	32.5	5.9	11.8	32.1	32.0
Gas load: 0.83 kg m^{-2} s^{-1}	72.2[b]	70.1	85.8	83.4	54.5	66.6	86.9	82.2
	47.3[c]	56.5	46.6	49.9	22.6	45.2	49.3	49.1
	18.3[d]	24.1	7.7	9.9	18.8	22.7	7.5	10.7
	59.8[e]	62.6	54.2	62.4	60.8	63.4	52.2	50.1
	4.9[f]	0.0	2.2	1.1	3.9	0.0	2.9	0.0
Gas load: 0.08 kg m^{-2} s^{-1}	7.4	11.1	16.2	21.9	4.8	5.3	14.6	22.9
	77.5	78.0	85.2	87.3	65.9	59.8	71.3	85.8
	28.2	42.6	24.7	33.8	18.2	20.5	22.3	35.1
	9.1	12.0	4.3	4.9	9.4	13.8	8.9	5.9
	40.2	47.7	63.2	30.8	38.1	25.2	37.0	39.8
	3.7	2.9	5.3	3.1	3.7	2.2	3.3	1.9
Electrolyte load, 4.4 kg m^{-2} s^{-1}	11.5	12.3	21.2	30.3	5.4	8.5	18.8	26.3
Gas load: 0.83 kg m^{-2} s^{-1}	72.3	73.5	81.8	86.1	58.5	61.8	80.0	83.2
	44.0	47.3	32.4	46.3	20.8	32.7	28.8	40.3
	16.8	23.2	7.2	7.5	14.9	20.0	7.2	8.2
	58.5	53.5	52.9	47.8	39.8	37.7	51.8	45.0
	4.8	0.0	4.9	2.2	9.5	0.0	5.6	2.1
Gas load: 0.08 kg m^{-2} s^{-1}	5.5	11.3	13.4	18.7	4.0	6.3	12.8	13.6
	67.1	81.7	81.7	85.3	63.9	68.7	80.8	82.3
	20.9	43.3	20.5	28.7	15.5	24.0	19.7	20.8
	10.3	9.7	4.6	4.9	8.7	10.9	4.7	4.5
	35.0	41.0	33.5	35.4	29.9	34.6	51.5	28.6
	4.3	3.4	4.8	7.5	3.4	3.3	8.5	2.0

Union Carbide graphite; bipole bed thickness = 15 mm; pressure = 1.4–2.2 atm absolute.
[a] Space–time yield (kg h^{-1} m^{-3}); [b] selectivity (%); [c] current efficiency for PO (%); [d] current efficiency for DBP (%); [e] current efficiency for hydrogen (%); [f] current efficiency for oxygen (%).

Table 3. Factorial experiment results

	Reactor outlet, 30° C				*Reactor outlet, 60° C*			
	0.4 kA m^{-2}		*1 kA m^{-2}*		*0.4 kA m^{-2}*		*1 kA m^{-2}*	
	0.2 M	*0.5 M*	*0.2 M*	*0.5 M*	*0.2 M*	*0.5 M*	*0.2 M*	*0.5 M*
Electrolyte load, 13.2 kg m^{-2} s^{-1}	11.30[a]	11.45	11.02	11.40	10.83	11.20	10.65	11.60
Gas load: 0.83 kg m^{-2} s^{-1}	8.6[b]	5.9	15.5	10.0	17.6	5.7	11.6	7.4
Gas load: 0.08 kg m^{-2} s^{-1}	11.23	11.58	10.96	11.35	10.86	11.40	10.25	11.45
	14.4	7.4	29.2	15.8	19.3	12.6	29.8	10.3
Electrolyte load, 4.4 kg m^{-2} s^{-1}	10.55	11.45	11.01	11.25	10.63	11.40	10.15	11.60
Gas load: 0.83 kg m^{-2} s^{-1}	9.2	6.6	22.8	10.8	18.2	7.9	25.7	9.2
Gas load: 0.08 kg m^{-2} s^{-1}	11.01	11.45	9.96	11.13	10.6	11.35	9.70	11.43
	29.4	7.3	36.1	18.7	25.0	10.8	29.1	17.7

Union Carbide graphite; bipole bed thickness = 15 mm; pressure = 1.4–2.2 atm absolute.
[a] pH value; [b] Specific energy consumption for PO (kW h kg^{-1}).

3.1. *Factorial effects of current, bromide concentration, temperature and flow*

In Tables 2–4 reactor performance is measured with respect to five independent variables (a–e) in terms of seven dependent variables listed in Table 1. Table 5 gives a summary of the analysis of variance of the data of Tables 2–4. Total reactor voltage in these runs varied from about 14 V at 0.4 kA m^{-2} to 40 V at 1 kA m^{-2}. These

Table 4. Factorial experiment results

	Reactor outlet, 30° C				*Reactor outlet, 60° C*			
	0.4 kA m^{-2}		*1 kA m^{-2}*		*0.4 kA m^{-2}*		*1 kA m^{-2}*	
	0.2 M	*0.5 M*	*0.2 M*	*0.5 M*	*0.2 M*	*0.5 M*	*0.2 M*	*0.5 M*
Electrolyte load, 13.2 kg m^{-2} s^{-1}	4.4[a]	8.2	4.4	2.5	3.6	6.2	5.9	1.8
Gas load: 0..83 kg m^{-2} s^{-1}	2.3[b]	0.0	2.2	0.1	2.3	0.0	3.8	0.2
	6.2[c]	11.5	25.7	1.7	5.3	3.0	27.2	0.8
	12.9[d]	19.7	32.3	4.3	11.2	9.2	36.9	2.8
Gas load: 0.08 kg m^{-2} s^{-1}	4.0	14.9	6.0	13.8	4.5	6.2	11.0	7.5
	10.4	0.7	2.9	2.9	0.0	3.9	7.7	4.1
	31.2	14.3	45.6	24.5	7.5	5.2	46.4	9.3
	45.6	29.9	54.5	41.2	12.0	15.3	65.1	20.9
Electrolyte load, 4.4 kg m^{-2} s^{-1}	2.1	3.2	3.5	4.0	1.5	2.7	3.0	4.5
Gas load: 0.83 kg m^{-2} s^{-1}	2.4	2.4	1.6	1.3	0.8	0.0	0.6	1.8
	8.5	4.5	21.9	12.4	1.3	4.4	15.5	4.2
	13.0	10.1	27.0	17.7	3.6	7.1	19.1	10.5
Gas load: 0.08 kg m^{-2} s^{-1}	6.0	3.4	4.2	4.9	3.0	3.0	3.8	3.9
	2.4	0.8	3.5	1.0	4.0	0.2	2.2	1.8
	16.9	5.1	48.2	27.5	4.5	2.6	29.8	16.1
	25.3	9.3	55.9	33.4	11.5	5.8	35.8	21.8

Union Carbide graphite; bipole bed thickness = 15 mm; pressure = 1.4–2.2 atm absolute.
[a] Current efficiency for BrO^-; [b] current efficiency for BrO_2^-; [c] current efficiency for BrO_3^-; [d] total current efficiency.

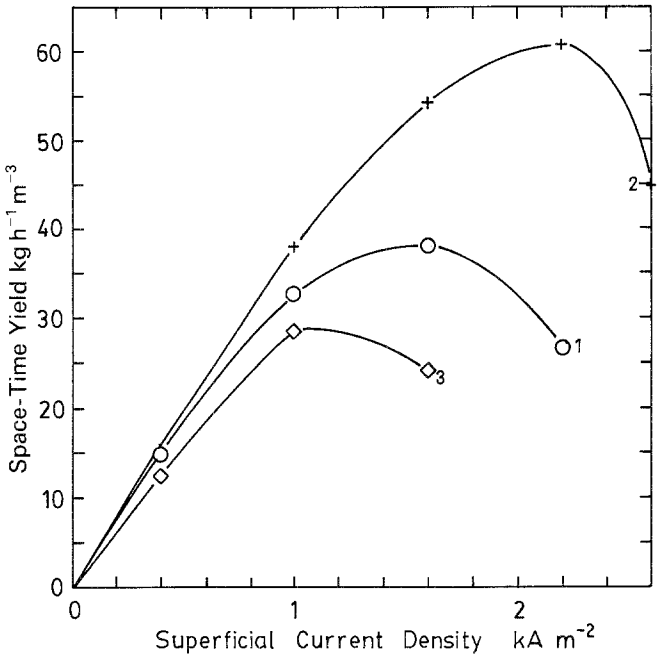

Fig. 3. Effect of current and gas flow on space–time yield for propylene oxide. Curve 1: gas flow, 1.01 min^{-1} (STP), 0.83 kg m^{-2} s^{-1}; pH range, 11.40–11.46. Curve 2: gas flow, 1.51 min^{-1} (STP), 1.25 kg m^{-2} s^{-1}; pH range, 11.45–11.60. Curve 3: gas flow, 2.01 min^{-1} (STP), 1.66 kg m^{-2} s^{-1}; pH range, 11.27–11.38. Graphite particle size, 1.2–1.7 mm; graphite type, UCAR; temperature, 28–35° C; pressure, 1.2–1.4 atm; NaBr concentration, 0.5 M; liquid load, 13.2 kg m^{-2} s^{-1}; bed thickness, 15 mm; superficial electrode area, 48 × 10^{-4} m^2.

values include voltage drop across five diaphragms, four bipole beds and two monopole beds. Reactor inlet pressure was in the range 1.5 to 2.2 bar (absolute) and outlet 1.1 bar (absolute).

The major effects on space–time yield for propylene oxide in Table 5 come from current and gas flow. Increased current increases the rate of Reaction 1 (up to the limit of bromide ion transfer), and this will result in an increased rate of propylene oxide formation as long as it is matched by the rate of propylene absorption into the electrolyte. Increased gas flow both raises the propylene transfer capacity of the beds and reduces current bypass by lowering the effective electrolyte conductivity.

The increase in selectivity with current implies a favourable balance for propylene oxide formation among Reactions 3, 4, 13 and 14 with increasing bromine generation rate. Between 0.4

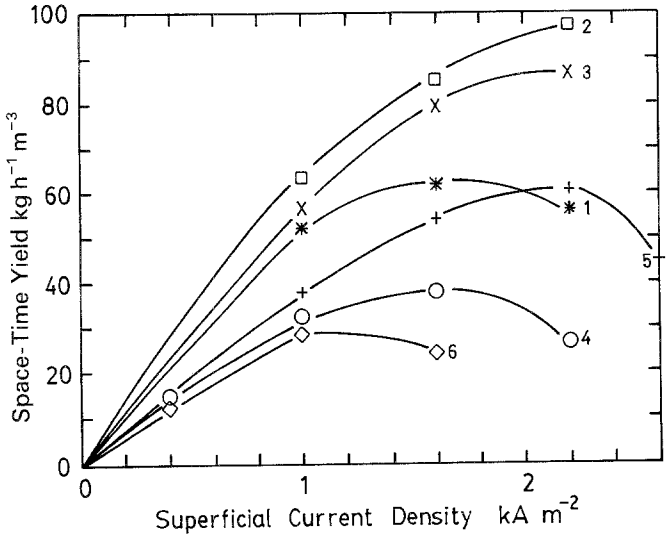

Fig. 4. Effect of bed thickness, current and propylene flow on the space–time yield for propylene oxide. Curve 1: bed thickness, 5 mm; gas flow, 1.01 min^{-1} (STP). Curve 2: 5 mm, 1.51 min^{-1} (STP). Curve 3: 5 mm, 2.01 min^{-1} (STP). Curve 4: 15 mm, 1.01 min^{-1} (STP). Curve 5: 15 mm, 1.51 min^{-1} (STP). Curve 6: 15 mm, 2.01 min^{-1} (STP). Graphite particle size, 1.2–1.7 mm; graphite type, UCAR; temperature, 28–35° C; pressure, 1.4–2.2 atm; NaBr concentration, 0.5 M; liquid flow, 0.31 min^{-1}; superficial electrode area, 45 × 10^{-4} m^2.

Table 5. Source table resulting from five-factor analysis of variance

Independent Variable	*Dependent variable*									
	Propylene oxide				*Current efficiency*					
	Space–time yield	*Selectivity*	*Current efficiency*	*Specific energy conspt.*	*Dibromopropane*	*Hydrogen*	*Oxygen*	*Hypobromite*	*Bromite*	*Bromate*
Temperature, I	0.26 (−)	427.8 (−)	685.4 (−)							381.1 (−)
Current, *A*	5.86 (+)	1758.3 (+)		336.7 (+)	562.0 (−)					1436.1 (+)
Concentration, *C*	0.49 (+)		744.0 (+)	875.7 (−)	37.2 (+)		60.5 (−)		26.7 (−)	1303.7 (−)
Electrolyte flow rate, *L*	0.39 (+)		350.5 (+)	89.1 (−)				72.9 (+)		
Propylene gas flow rate, *G*	1.65 (+)		1804.5 (+)	379.5 (−)	300.8 (+)	1815.0 (+)		46.5 (−)	22.2 (−)	896.9 (−)
$A \times L$[a]	0.19									
$A \times G$	0.47				83.4					222.0
$A \times C$					20.6					636.6
$T \times A$			399.8	99.4						
Residual (d.f.)[b]	0.40 (24)	647.3 (29)	551.8 (26)	302.1 (26)	65.9 (26)	2249.3 (30)	111.5 (30)	119.4 (29)	108.4 (29)	848.0 (25)
Total	9.71	2833.4	4536.0	2082.5	1069.9	4064.3	172.0	304.5	157.3	5724.4

[a] First order interaction, measuring the extent to which the effect of one factor, in this case current, depends upon the value of the other factor, electrolyte flow rate.
[b] d.f. = degrees of freedom.
The numbers reported above are the sums of squares.

Table 6. The effect of current and propylene gas load on the space–time yield, selectivity and energy consumption for propylene oxide and current efficiencies

Current density ($kA\,m^{-2}$)	*Outlet pH*	*Gas load* ($kg\,m^2\,s$)	*Space-time* ($kg\,h^{-1}\,m^{-3}$)	*Energy consumption* ($kW\,h^{-1}\,kg^{-1}$)	*Current efficiency (%)*				*Selectivity (%)*
					Propylene oxide	*Dibromopropane*	*Oxygen*	*Hydrogen*	
0.4	11.45	0.83	14.8	5.9	56.5	24.1	0.0	62.6	70.1
1.0	11.42	0.83	32.6	10.0	49.9	9.9	1.1	62.4	83.5
1.6	11.40	0.83	38.0	17.3	36.4	7.0	3.6	56.9	83.9
2.2	11.46	0.83	26.6	40.1	18.6	7.0	4.5	58.3	72.5
1.0	11.50	1.52	38.0	9.2	58.2	12.9	1.6	59.4	81.8
1.6	11.53	1.52	54.2	13.1	51.9	12.1	3.0	62.1	81.1
2.2	11.60	1.52	60.7	17.4	42.3	8.6	3.8	58.0	83.1
2.6	11.45	1.52	44.8	31.2	26.4	8.4	4.9	56.9	76.0
0.4	11.35	1.66	12.4	7.0	47.6	29.6	–	–	61.8
1.0	11.27	1.66	28.5	12.7	43.6	13.9	2.9	56.3	75.8
1.6	11.38	1.66	24.2	31.1	23.2	7.7	5.5	60.9	75.2

Conditions: graphite particle size = 1.2–1.7 mm; liquid load = $13.2\,kg\,m^{-2}\,s^{-1}$; graphite type = Union Carbide; pressure = 1.4–2.2 atm; temperature = 28–35° C; bed thickness = 15 mm; concentration = 0.5 M.

and 1 kA m^{-2} the rate of production of dibromopropane is nearly independent of current density. The higher current apparently goes to increase the rate of production of propylene oxide and of bromate.

The positive effect of liquid and gas flow on current efficiency for propylene oxide is probably a reflection of a corresponding improved capacity for propylene transfer and decreased current bypass. There may also be an improvement in intra-cell mixing. Bromide concentration has an unexpected positive effect on efficiency for propylene oxide which may be due to improved transfer to Br^- to the anode, as seen by the decrease in current efficiency for oxygen.

Specific energy for propylene oxide decreases with increased bromide concentration, liquid flow and gas flow due to the corresponding increases in current efficiency. An increase in current raises specific energy by its effect on the reactor voltage.

The weak negative effect of temperature on space–time yield, selectivity and current efficiency for propylene oxide may be the result of several factors: a reduction in propylene solubility (from about 5×10^{-3} M at 30° C to 2×10^{-3} M at 60° C), an increase in electrolyte conductivity and a change in the relative reaction rates in the process. There may also be subtle effects from changes in electrolyte outlet pH as recorded in Table 3. Variations in pH affect the bromine–hypobromite equilibrium, the rate of formation of dibromopropane and the rate of hydrolysis of propylene oxide to propylene glycol.

Current efficiency for hydrogen in these runs varies from about 25 to 60%. The lost hydrogen efficiency may be attributed to current bypass, plus cathode reduction of bromine species (Br_2, OBr^-) and oxygen. The data are insufficient to separate these effects, but current bypass is likely to be the major contributor.

3.2. *Current and gas flow*

The results of more comprehensive experiments on the effect of current and propylene gas flow on the space–time yield for propylene oxide are shown in Fig. 3. Table 6 gives corresponding data on some other dependent variables measured in these runs. In Fig. 3 the space–time yield passes a maximum with respect to both current and gas flow. This probably results from the interaction of current with the effects of gas flow on the propylene transfer-limited current density, effective electrolyte conductivity and lateral mixing in the cells. The rates of both oxygen and dibromopropane production increase with current as the anode potential rises and Reaction 3 becomes constrained by propylene transfer. In Table 6 the total of the anode current efficiencies for PO, DBP and oxygen decreases with rising current, from above to far below the current efficiency for hydrogen on the cathodes. These discrepancies in current exceed the experimental error and are presumably due to the generation and destruction of other species within the reactor such as hyprobromite, bromite, bromate, propylene glycol, etc., as indicated in Table 4.

3.3. *Bed thickness*

The effect of decreasing the thickness of each bipole bed from about 15 to 5 mm is shown in Fig. 4 and Table 7. The corresponding increase in maximum space–time yield for propylene oxide is 1.6 times at $G = 1.01\,\mathrm{min}^{-1}$ to three times at $G = 2.01\,\mathrm{min}^{-1}$. There is a drop in current efficiency for propylene oxide which is presumably due to increased current bypass in the thinner bed. Higher gas flow counters the effect of lower bed thickness by decreasing the effective conductivity of the electrolyte. It should also be noted that the gas and liquid loads in the 5 mm beds are about three times higher than those in the 15 mm beds at corresponding fluid flows. The average voidage is also higher in the 5 mm bed than the 15 mm bed. Such increased loadings have substantial effects on mass transfer, mixing and residence time in the reactor.

3.4. *Electrode material*

Findings from experiments carried out with different graphite materials in the fixed beds are presented in Table 8. Changing the graphite from Union Carbide to Ultra Carbon yields lower space–time yield, current efficiency and selectivity for propylene oxide. These results are

Table 7. Effect of bed thickness, superficial current density and propylene gas flow rate on the space–time yield for propylene oxide

Gas flow rate at STP ($l\,min^{-1}$)	*Bed thickness, 5 mm*			*Bed thickness, 15 mm*				
	1.0 kA m^{-2}	*1.6 kA m^{-2}*	*2.2 kA m^{-2}*	*0.4 kA m^{-2}*	*1.0 kA m^{-2}*	*1.6 kA m^{-2}*	*2.2 kA m^{-2}*	*2.6 kA m^{-2}*
2.0	56.9[a]	79.1	86.5	12.4	28.5	24.2	–	–
	10.73[b]	10.98	11.03	11.35	11.27	11.38	–	–
	69.5[c]	74.4	75.5	61.8	75.8	75.2	–	–
	31.3[d]	27.2	21.6	47.6	43.6	23.2	–	–
	13.8[e]	9.3	7.1	29.6	13.9	7.7	–	–
	10.2[f]	14.2	15.5	5.6	14.3	12.3	–	–
1.5	63.4	85.2	97.2	–	38.0	54.2	60.7	44.8
	10.98	10.92	10.83	–	11.50	11.60	11.60	11.45
	73.5	71.2	72.0	–	81.8	81.1	83.1	76.0
	34.9	29.3	24.3	–	58.2	51.9	42.3	26.4
	12.6	11.8	9.5	–	12.9	12.1	8.6	8.4
	11.35	15.3	17.4	–	19.0	27.0	30.3	22.3
1.0	52.1	61.7	56.2	14.8	32.6	38.0	26.6	–
	10.03	10.87	10.76	11.45	11.40	11.40	11.46	–
	72.6	67.1	57.8	70.1	83.5	83.9	72.5	–
	28.7	21.2	14.0	56.5	49.9	36.4	18.6	–
	10.8	10.4	10.2	24.1	9.9	7.0	7.0	–
	9.3	11.0	10.1	7.4	16.2	19.0	13.3	–

Conditions: graphite particle size = 1.2–1.7 mm; liquid load = 13.2 kg m^{-2} s^{-1}; graphite type = Union Carbide; pressure = 1.4–2.2 atm; temperature = 28–35° C; area = 48.4 cm^2; concentration = 0.5 M.
[a] Space–time yield (kg h^{-1} m^{-3}); [b] pH value; [c] selectivity (%); [d] current efficiency for PO; [e] current efficiency for DBP; [f] production rate of PO.

probably due to the higher porosity of the Ultra Carbon graphite, but the graphite properties are not defined well enough to be more specific on this point. The porous graphite provides dead space where localized low pH regions caused by poor mass transfer can develop, allowing undesirable reactions to take place which reduce the selectivity and space–time yield for propylene

Table 8. The effect of different carbon types on the space–time yield for propylene oxide

	Space–time yield (kg h^{-1} m^{-3})	*Production rate of PO (cm^3 h^{-1})*	*Current efficiency for PO (%)*	*Current efficiency for DBP (%)*	*Selectivity (%)*
Union Carbide					
13.2 kg m^{-2} s^{-1}[a]; 0.83 kg m^{-2} s^{-1}[b]	32.5	16.2	49.9	9.9	83.5
13.2 kg m^{-2} s^{-1}[a]; 0.08 kg m^{-2} s^{-1}[b]	21.9	11.0	33.8	4.9	87.3
4.4 kg m^{-2} s^{-1}[a]; 0.83 kg m^{-2} s^{-1}[b]	30.3	15.1	46.3	7.5	86.1
4.4 kg m^{-2} s^{-1}[a]; 0.08 kg m^{-2} s^{-1}[b]	18.7	9.4	28.7	4.9	85.4
Ultra Carbon					
13.2 kg m^{-2} s^{-1}[a]; 0.83 kg m^{-2} s^{-1}[b]	25.6	12.8	39.4	10.2	79.5
13.2 kg m^{-2} s^{-1}[a]; 0.08 kg m^{-2} s^{-1}[b]	18.6	9.3	28.6	6.2	82.3
4.4 kg m^{-2} s^{-1}[a]; 0.83 kg m^{-2} s^{-1}[b]	18.9	9.5	29.1	8.7	77.0
4.4 kg m^{-2} s^{-1}[a]; 0.08 kg m^{-2} s^{-1}[b]	11.1	5.5	17.0	6.0	73.8

Conditions: concentration = 0.5 M; current density = 1 kA m^{-2}; temperature = 28–34° C; bed thickness = 15 mm; pressure = 1.4–2.2 atm.
[a] Liquid load; [b] gas load.

oxide. The lower space–time yield for propylene oxide coincides with an increased current efficiency for dibromopropane.

4. Conclusions

Propylene oxide was synthesized in a 'flow-by' bipolar trickle-bed electrochemical reactor. The reactor was operated with a single pass of propylene gas and sodium bromide electrolyte solution at an average pressure around 1.5 bar absolute. The performance of the bipole bed reactor was governed by the combined effects of electrolyte concentration, superficial current density, temperature, fluid flows, bed thickness and electrode material. In particular, the space–time yield for propylene oxide was increased by increased current density, increased gas flow and decreased bed thickness.

Under conditions of these experiments the bipole bed reactor gave fair selectivity for propylene oxide ($\sim$ 55–85%). It is suggested that the low current efficiency ($\sim$ 15–55%) and high specific energy ($\sim$ 6–60 kW h kg^{-1}) is largely accounted for by current bypass and losses due to secondary generation of bromate ($\sim$ 10–45%), oxygen ($\sim$ 0 to 8%) and diprobromopropane ($\sim$ 5–20%) plus possible losses of intermediate bromine species of cathodic reduction.

Despite the low current efficiency the space–time yields for propylene oxide obtained in these runs ($\sim$ 10–100 kg m^{-3} h^{-1}) are relatively high compared to previously reported results of work on this process near ambient pressure (up to 10 kg m^{-3} h^{-1}). The good space–time yields are attributed to the high capacity for propylene absorption and specific surface of the bipole trickle-bed electrodes.

Acknowledgements

The experimental part of this work was financed by the Natural Sciences and Engineering Research Council of Canada. The authors also thank Erco Industries and the University of British Columbia for support in preparation of the manuscript.

References

[1] M. Fleischmann, J. W. Oldfield, and C. L. K. Tennakoon, *IChemE. Symp. Series* **37** (1971) 153.
[2] F. Beck, XXIVth International Congress of Pure and Applied Chemistry, Vol. 5, London, Butterworth (1973) p. 111.
[3] C. J. H. King, K. Lister, and R. E. Plimley, *Trans. Instn. Chem. Engrs.* **53** (1975) 20.
[4] J. Ghoroghchian, R. E. W. Jannson, and D. Jones, *J. of Appl. Electrochem.* **7** (1977) 437.
[5] A. V. Boussoulengas, S. Edhai, and R. E. W. Jannson, *Chem. and Ind.* **60** (1979) 670.
[6] P. Robertson, P. Cetton, D. Matic, F. Schwager, A. Storck and N. Ibl, *AIChE Symp. Series*, **75** (1979) 115.
[7] T. Bejerano, S. Germain, F. Goodridge and A. R. Wright, *Trans. Instn. Chem. Engrs.* **58** (1980) 28.
[8] K. G. Ellis and R. E. W. Jansson, *J. Appl. Electrochem.* **11** (1980) 531.
[9] *Idem, ibid.* **13** (1983) 651.
[10] R. Alkire, *J. Electrochem. Soc.* **120** (1973) 900.
[11] C. Oloman, *ibid.* **126** (1979) 1885.
[12] A. Manji, MASc Thesis, University of British Columbia, December 1984.
[13] M. H. Hashmi and A. A. Ayaz, *J. Anal. Chem.* **35** (1963) 908.